CHEMICAL ENGINEERING TRANSACTIONS
VOL. 43, 2015
A publication of AIDIC
The Italian Association of Chemical Engineering
Online at www.aidic.it/cet
Chief Editors: Sauro Pierucci, Jiří J. Klemeš

ISBN 978-88-95608-34-1; **ISSN** 2283-9216
DOI: 10.3303/CET1543141

Microstructural Properties and HDS Activity of CoMo Catalysts Supported on Activated Carbon, Al_2O_3, ZrO_2 and TiO_2

Karel Soukup, Martin Procházka, Luděk Kaluža*

Institute of Chemical Process Fundamentals of the ASCR, v. v. i.; Rozvojová 135; 165 02 Prague 6–Suchdol; Czech Republic
kaluza@icpf.cas.cz

Unconventional supports of CoMo catalysts, such as activated carbon, ZrO_2 and TiO_2 and conventional Al_2O_3 support in the form of cylindrical extrudates were studied using inverse gas chromatography with single pellet-string column (SPSC) configuration, high pressure mercury porosimetry and nitrogen adsorption methods to assess both the transport and textural characteristics. The supports were saturated from an aqueous slurry of MoO_3. MoO_3 supported catalysts were promoted from the aqueous slurry of $CoCO_3.Co(OH)_2$. The transport and textural parameters of all CoMo catalysts prepared in their both oxidic and sulfide form were compared with that of the parent supports. It was concluded that the support effect, represented in the present work by surface area, CoMo loading and mainly the mean transport-pore radius, govern resultant activity of CoMo catalysts. The increasing mean transport-pore radii either of the support or of the sulfide catalyst correlated well qualitatively with the increasing activity in HDS of 1-benzothiophene in the order: $ZrO_2 \sim TiO_2 < Al_2O_3 < C$. The unconventional ZrO_2- and TiO_2-supported systems exhibited low microstructural changes in terms of textural and transport characteristics after deposition of CoMo and low HDS activities. In contrast, Al_2O_3- and C-based systems revealed significant changes in microstructure after deposition of the CoMo phases onto the supports and high HDS activities. The activated carbon supported CoMo catalyst exhibited the highest HDS activity and the mean transport-pore radius despite the highest volume of micropores.

1. Introduction

Cobalt-molybdenum sulfides supported on gamma-Al_2O_3 represent conventional catalysts for industrial scale hydrodesulfurization (HDS) reaction of crude-oil fractions (Toulhoat and Raybaud, 2013). Moreover, they have been recently studied for hydrodeoxygenation reactions of bio oils (Baladincz et al., 2012) or lignins (Jongerius et al., 2012) as renewable feedstocks for production of fuels. Furthermore, alternative supports (Breysse et al., 2003) and/or methods of CoMo deposition (Kaluža et al., 2013) have been researched to innovate the hydroprocessing (Leliveld and Eijsbouts, 2008). Nevertheless, most of the scientific papers in the field deals with catalysts and supports in the form of grains despite the fact that industrial scale processes require shaped forms such as extrudates or tablets. Only limited effort, up to the authors best knowledge, was devoted to shaped form of supports and catalysts. For example, the CoMo deposition onto shaped supports was followed by electron probe microanalysis, EMPA, UV-vis and Raman spectroscopy, Tomographic Energy Dispersive Diffraction or Multinuclear Magnetic Resonance; the references are given in (Kaluža and Zdražil, 2009).
The purpose of the present work is to report briefly on the subsequent deposition of MoO_3 and $CoCO_3$ onto the extrudates of activated carbon (Kaluža and Zdražil, 2001), Al_2O_3 (Kaluža et al., 2005), ZrO_2 and TiO_2 (Kaluža and Zdražil, 2009) by water assisted spreading method. The deposition and pre-activation by sulfidation were followed by specific microstructural analyses based on nitrogen physisorption, high-pressure mercuric porosimetry and inverse gas chromatography measurements. Though the inverse gas chromatography method is broadly used in characterization of washcoat automotive catalysts (Kolaczkowski,

Please cite this article as: Soukup K., Prochazka M., Kaluza L., 2015, Microstructural properties and hds activity of como catalysts supported on activated carbon, al2o3, zro2 and tio2, Chemical Engineering Transactions, 43, 841-846 DOI: 10.3303/CET1543141

2003), it has not been exploited and reported in the literature related to HDS catalysts so far. The activities of the sulfided catalysts were determined in HDS reaction of 1-benzothiopene.

2. Experimental

2.1 Supports and Catalysts

Extrudates of activated carbon (Norit N.V., Norit RX3 extra), Al_2O_3 (Alfa Aesar, product no. 043832), ZrO_2 (Alfa Aesar, product no. 043815) and TiO_2 (Alfa Aesar, product no. 044429) of the same external diameter corresponding to 3.2 mm were selected and cut to the uniform length of 5 mm. Thereafter, the extrudates were washed with HPLC grade water at 60 °C until the water was clear of solid dust. 160 pieces of each was immersed into aqueous slurry of MoO_3 (Fluka, p.a., product no. 69850, finely pulverized in a planetary mill for 8 h) for their saturation. In the solid part, the nominal content of MoO_3 was 38 wt. % and 28 wt. % for the high-surface-area active carbon and medium-surface-area oxidic supports, respectively. The mixtures were stirred at laboratory temperature for 7 days, heated under reflux condenser at 95 °C for 8 hour, and again stirred at laboratory temperature for other 7 days. The extrudates were separated from the slurry by decantation and dried in vacuum rotary evaporator at 95 °C for 4 h. Then, the extrudates were immersed into aqueous slurry of $CoCO_3.Co(OH)_2$ (Merck, p.a., product no. 2551, finely pulverized in a planetary mill for 8 h) corresponding to nominal content of CoO 10 wt.% in the solid part of the mixtures. The impregnation was performed analogously as it was described for MoO_3 above. Selected extrudes were half cut and analyzed by EMPA. Uniform ratio Co/Mo was found through the extrudates. The actual loadings of the metals are summarized in Table 1. Total loading CoO + MoO_3 (L) is shown in Figure 1. The actual saturation loadings were similar as we observed previously over C (Kaluža and Zdražil, 2001), Al_2O_3 (Kaluža et al., 2005), ZrO_2 and TiO_2 (Kaluža and Zdražil, 2009) supports. Prior to microstructural analysis, the selected catalysts were presulfided as it is described below and flushed by N_2 at 400 °C for 1 h and at laboratory temperature for 3 additional days.

2.2 Texture analysis

The physical adsorption of nitrogen, the high-pressure mercury porosimetry and the helium pycnometry were used for determination of the texture characteristics of prepared catalysts. The BET surface area S_{BET}, the mesopore surface area S_{meso} and the micropore volume V_{micro} were evaluated from the nitrogen physical adsorption-desorption isotherms measured at 77 K using both the ASAP2020M and ASAP2050M instruments (Micromeritics, USA) by two independent methods. The modified BET equation (Schneider, 1995) and the *t*-plot were constructed by means of the Leclux-Pirrard standard isotherm (Schneider et al., 2008). The high-pressure mercury porosimetry performed on AUTOPORE III instrument (Micromeritics, USA) were used for determination of the the apparent density, ρ_{Hg}, and the pore-size distribution curves. Skeletal density ρ_{He} was determined on the AccuPyc 1920 instrument (Micromeritics, USA) and porosity ε of all studied samples was determined according to $\varepsilon = 1 - (\rho_{Hg}/\rho_{He})$. To guarantee the precision of the obtained data the purity of the used nitrogen and helium (Linde Technoplyn, a.s.) was grade of 99.9995 %. Before the measurements, all samples were evacuated at 110 °C for 12 h.

2.3 Transport properties

The inverse gas chromatography setup (Figure 2) consists of a chromatographic column, thermal conductivity detector (Micro-TCD 10-955, Gow-Mac Instruments Co., USA), calibrated mass flow-meters/controllers (Brooks 5850S, Brooks Instruments, the Netherlands), and six port sampling valve (sample volume 250 μl) with an electric actuator (Valco Instruments Co. Inc., USA). Two columns with lengths of 50 cm and 25 cm and identical inner diameter (4.2 mm) were packed with tested extrudates. All chromatographic measurements were performed at laboratory temperature and pressure. Argon, nitrogen and helium were selected both as

Table 1: Loadings and HDS activities of CoMo catalysts

CoMo supports	C	Al_2O_3	ZrO_2	TiO_2
CoO [wt.%]	2.0	2.1	1.7	2.3
MoO_3 [wt.%]	30.0	15.2	6.5	10.2
k(EB) [mmol(EB) g^{-1} h^{-1}]	749	383	122	142
k(EB,CoMo)/k(EB,Mo)	8.3	7.3	4.1	3.6
ρ(Packing) [g cm^{-3}]	0.62	0.70	1.24	0.90
k(EB) [mmol(EB) cm^{-3} h^{-1}]	464	268	151	128

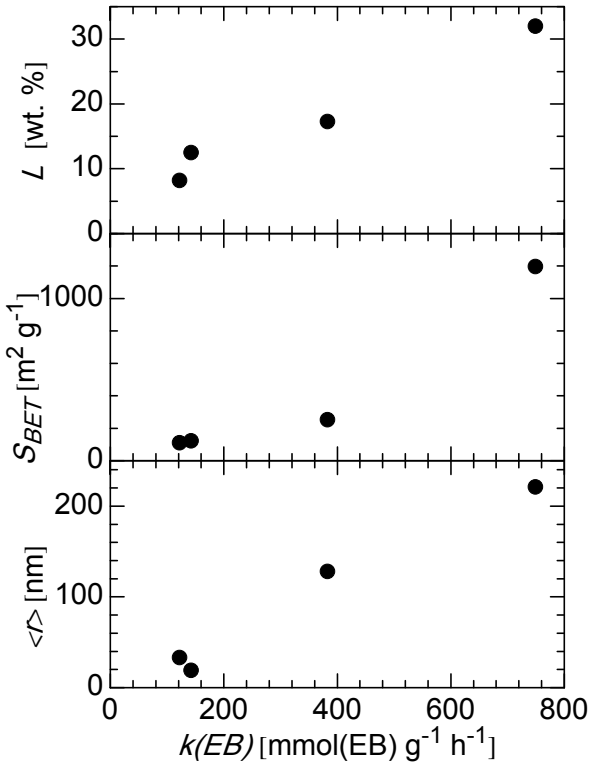

Figure 1: Empiric correlation of the CoMo loadings L, support surface area S_{BET} and support mean transport-pore radius <r> with the HDS activity k(EB)

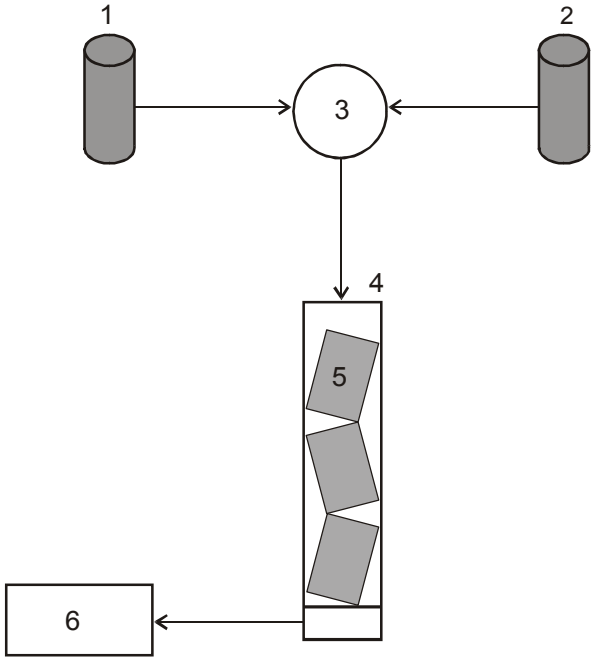

Figure 2: Inverse gas chromatography setup. (1): carrier gas source; (2): tracer gas source; (3): six-way sampling valve; (4): chromatographic column; (5): tested samples; (6): PC with digital data logger

carrier and tracer gases. Five different carrier gas flow rates were used: 10, 20, 30, 50 and 90 cm^3 min^{-1}. Approximately 3,000 response points from the TCD detector were recorded on a digital data logger. After zero-line correction (less than 0.1 % of the maximum response height) about 90 uniformly distributed experimental points were normalized to the maximum of the tracer concentration. The final response signals were obtained by averaging three individual peaks for each carrier gas flow rate and carrier/tracer pair of gases. The transport characteristics were evaluated from these averaged response signals.

During measurements, a pulse of tracer gas was injected into the carrier-gas stream, which flowed at constant flow rate through the column. The tracer concentration was measured at the column outlet by the TCD detector. The recorded outlet response signal was then analyzed. Analysis of outlet peaks was based on the transport processes inside the column. The transport model by Kubín-Kučera (Kučera, 1965) has been usually used. Matching of column response signals with the model equations is possible to perform in the time domain (Schneider, 1984). The Kubín-Kučera model describes intracolumn processes, such as convection and axial dispersion of the tracer band, transport of the tracer through a laminar film around the packing particles, diffusion into the pore structure and adsorption (for adsorbable tracer gas) on the internal surface of porous packing as well extra-column effects account for processes upstream and downstream of the column. It has been suggested (Šolcová et al., 2006) that these processes can be included in the time-domain matching through application of the convolution theorem.

2.4 HDS of 1-benzothiophene

The HDS of 1-benzothiophene (BT) was performed at 360 °C and 1.6 MPa over catalyst grain fraction 0.16-0.32 mm in fixed-bed tubular flow micro-reactor (Kaluža et al., 2013). Before the measurements, the catalysts were presulfided in-situ by a H_2S/H_2 mixture (1:10) at atmospheric pressure with the following temperature program: ramp 6 °C min^{-1} to 400 °C and dwell 1 h at 400 °C. The composition of the feed was 16 kPa of BT, 200 kPa of decane and 1384 kPa of hydrogen. The catalyst charge, W, was 0.02-0.2 g depending on the catalyst activity and it was diluted with an inert corundum. The reaction was run at three feed rates of BT, F(BT): 7.7 mmol h^{-1}, 10.3 mmol h^{-1} and 15.5 mmol h^{-1}. Steady state was reached in 30 min after each change in the feed rate. The reaction mixture was analyzed on a gas chromatograph. Dihydrobenzothiophene (DH)

and ethylbenzene (EB) were identified in the reaction products. The yields of EB, y(EB) was defined as y(EB) = n(EB)/n_0(BT), where n_0(BT), n(EB), are the initial and final number of moles. The empirical pseudo-first-order rate constant and ethylbenzene formation *k(EB)* was calculated from the dependence of y(EB) within the range 0.05-0.95 on space time W/F and it was normalized per unit weight of sulfided catalyst. The promotion effect of Co was defined as a ratio of the activity of CoMo catalyst and its Mo counterpart. For the purpose of industrially meaningful comparison, the packing density, ρ(Packing), of the tested catalysts was determined on an analytical balance in a 2-mL measuring cylinder with inert diameter of 8 mm after five-time dabbing off. Packing densities and volume normalized activities are summarized in Table 1.

3. Results and Discussion

Texture characteristics of all prepared catalysts are summarized in Table 2. It is evident that the inner surface area expressed in terms of the both total S_{BET} area and S_{meso} area for all catalysts reveals somewhat lower values compared to those of the parent supports. This is probably caused by partial filling of the pores of support by the deposited phase affecting both micropores and mesopores. The most significant decline can be recognized in the line of the most microporous activated carbon (S_{BET} = 1196 $m^2 g^{-1}$), CoMo/C (S_{BET} = 477 $m^2 g^{-1}$) and $CoMoS_2$/C (S_{BET} = 521 $m^2 g^{-1}$). On the other hand, for the groups of ZrO_2 and TiO_2 based catalysts the texture characteristics remain almost unchanged with the parent supports.

The gas diffusion transport taking place in the pores of tested catalysts during the gas chromatographic measurements was described by means of the Mean Transport-Pore (MTPM) Model (Schneider, 1978). In this model description, the transport-pores are visualized as the bundles of cylindrical capillaries with radii distributed around the mean (integral) transport-pore radius, <*r*>. MTPM takes also into account their porosity, ε_t, and tortuosity, q_t (both of them are included in the ψ material parameter according to $\psi = \varepsilon_t/q_t$). The optimized transport parameters for all catalysts are summarized in Table 2. In agreement with the texture analysis (see above), it was found that transport properties of ZrO_2 as well as TiO_2-based catalysts in terms of their transport parameters were changed only slightly. Contrary to this finding, the most significant changes considering the transport parameters $\langle r\rangle\psi$ were identified in the line of Al_2O_3 ($\langle r\rangle\psi$ = 12.2 nm), CoMo/Al_2O_3 ($\langle r\rangle\psi$ = 7.24 nm) and $CoMoS_2$/Al_2O_3 ($\langle r\rangle\psi$ = 1.96 nm). The changes could be connected with partial corrosion of Al_2O_3 surface by interaction with Mo species during impregnation to form Anderson-type heteropolycomplexes as it was suggested elsewhere (Carrier et al., 2003). Nevertheless, transport parameters ψ including the influence of the transport-pore porosity and tortuosity do not change so considerably in any line of catalysts.

Figure 3 compares qualitatively the calculated mean transport-pore radii (determined as $\langle r\rangle = (\langle r\rangle\psi)/\psi$, here marked with an arrow) with the pore-size distributions (PSD) obtained from high-pressure mercury porosimetry (solid line). It can be clearly seen that all samples show bidispersed pore structure (revealing two maxima on the PSD curve). In most cases, the mean transport-pore radii are either positioned between peaks of the PSD closer to the peak for wider pores (corresponding to meso- and macro- pores) or correspond exactly with the maximum of the peak for wider pores. It follows that the gas diffusion transport in tested catalysts takes place predominantly through a set of wider pores and the role of narrower pores (micropores) depends on their total amount and size. Despite the fact that C based samples exhibited the highest V_{micro} and differences in PSD curves, they possessed the highest <*r*> and HDS activities *k(EB)*.

Table 2: Texture and transport characteristics

Sample	S_{BET} [$m^2 g^{-1}$]	S_{meso} [$m^2 g^{-1}$]	V_{micro} [$mm^3 g^{-1}$]	ρ_{He} [g cm^{-3}]	ρ_{Hg} [g cm^{-3}]	ε [–]	$\langle r\rangle\psi$ [nm]	ψ [–]	<*r*> [nm]
Al_2O_3	253	155	54	3.17	0.41	0.87	12.20	0.096	128
CoMo/Al_2O_3	259	158	57	3.14	0.77	0.76	7.24	0.105	69
$CoMoS_2$/Al_2O_3	170	110	32	2.20	1.96	0.39	1.96	0.049	40
ZrO_2	111	69	28	5.38	2.11	0.61	3.37	0.101	33
CoMo/ZrO_2	90	55	20	4.73	2.08	0.56	2.65	0.093	29
$CoMoS_2$/ZrO_2	84	56	18	4.69	1.97	0.58	2.78	0.124	23
TiO_2	123	76	27	3.64	1.44	0.60	2.69	0.139	19
CoMo/TiO_2	120	76	26	3.81	1.61	0.58	2.69	0.100	27
$CoMoS_2$/TiO_2	100	68	18	3.70	1.70	0.54	2.55	0.094	27
C	1196	517	369	2.13	0.66	0.69	13.80	0.062	221
CoMo/C	477	199	150	2.39	1.00	0.58	14.50	0.073	200
$CoMoS_2$/C	521	214	159	2.92	0.92	0.68	8.24	0.086	96

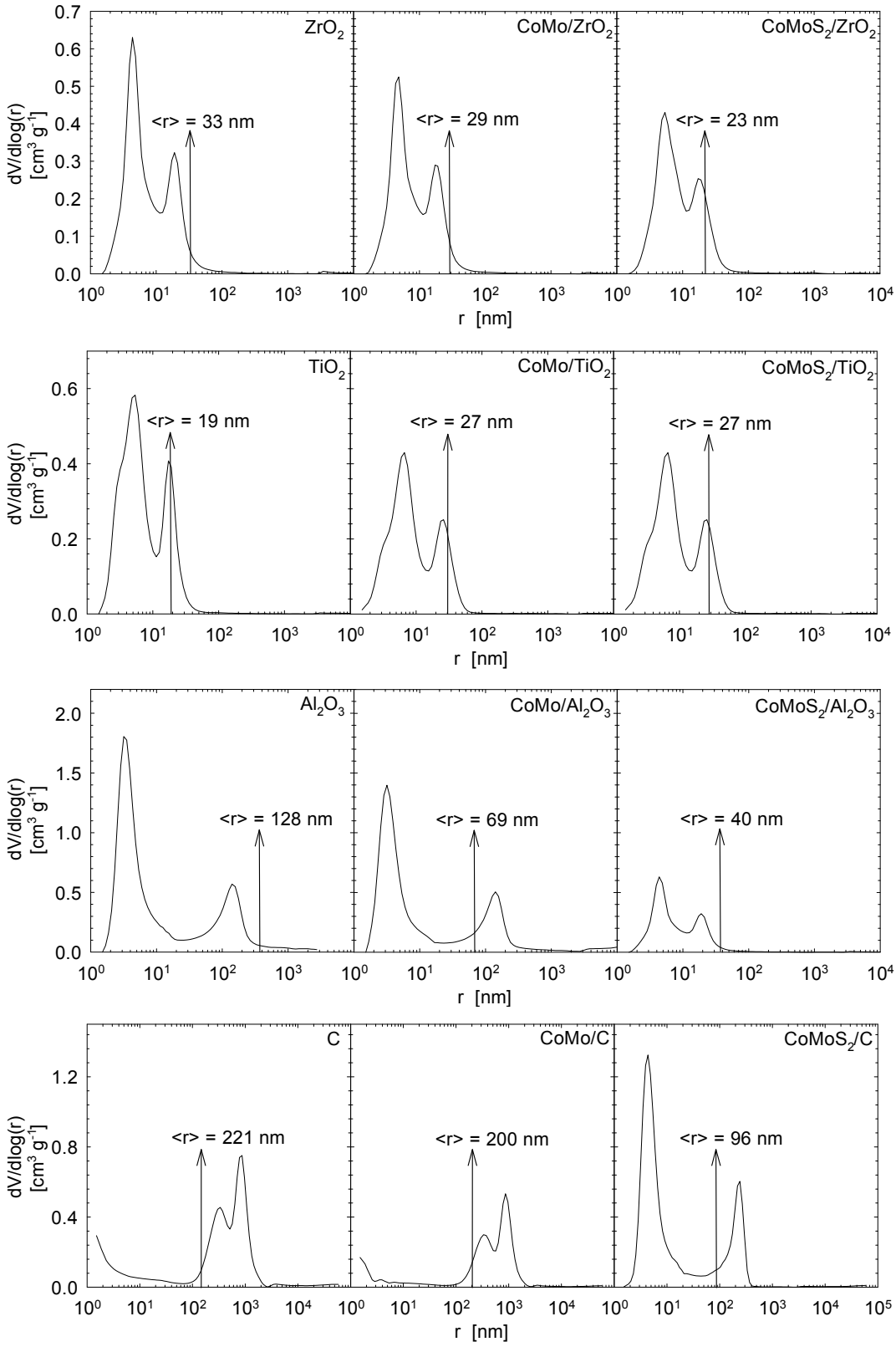

Figure 3: Comparison of the pore-size distribution curves (solid line) with the mean transport-pore radii (arrow) for all tested samples

4. Conclusions

It was concluded that the support effect, represented in the present work by S_{BET}, L and mainly the mean transport-pore radius $\langle r \rangle$, govern resultant activity of CoMo catalysts. The increasing mean transport-pore radii either of the support or of the sulfide catalyst correlated well qualitatively with the increasing activity in HDS of 1-benzothiophene in the order: $ZrO_2 \sim TiO_2 < Al_2O_3 < C$ (Figure 1). Nevertheless, according to the both microstructural analysis and HDS activity study, the supports and catalysts could be selected into two main groups. The first group, ZrO_2- and TiO_2-based systems, exhibited low microstructural changes in terms of textural and transport characteristics after deposition of CoMo (both in oxidic and sulfide stage) onto the supports, relatively narrow mean transport-pore radii between 19-33 nm, and low HDS activities of CoMo catalysts (both weight and volume normalized activities). In contrast, the second group, Al_2O_3- and C-based systems, revealed significant changes in microstructure after deposition of the CoMo phases onto the supports, but exhibited wider mean transport-pore radii ranging from 40 to 221 nm, and more than 1.8 times higher HDS activities of CoMo catalysts than the first group. The activated carbon supported CoMo catalyst exhibited the highest HDS activity and the mean transport-pore radius despite the highest volume of micropores, which emphasized relevancy of further research. It was corroborated that the inverse gas chromatography represents valuable method for evaluation of supported catalysts.

Acknowledgement

The financial support of the Czech Science Foundation (grant number P106/11/0902) is acknowledged.

References

Baladincz P., Tóth C., Hancsók J., 2012, Production of diesel fuel via hydrogenation of rancid lard and gas oil mixtures, Chemical Engineering Transactions, 29, 1237-1242.

Breysse M., Afanasiev P., Geantet C., Vrinat M., 2003, Overview of support effects in hydrotreating catalysts, Catal. Today, 86, 5-16.

Carrier X., Lambert J.F., Kuba S., Knözinger H., Che M., 2003, Influence of ageing on MoO_3 formation in the preparation of alumina-supported Mo catalysts, J. Mol. Struct., 656, 231-238.

Jongerius A.L., Jastrzebski R., Bruijnincx P.C.A., Weckhuysen B.M., 2012, CoMo sulfide-catalyzed hydrodeoxygenation of lignin model compounds: An extended reaction network for the conversion of monomeric and dimeric substrates, J. Catal., 285, 315-323.

Kaluža L., Zdražil M., 2001, Carbon-supported Mo catalysts prepared by a new impregnation method using a MoO_3/water slurry: Saturated loading, hydrodesulfurization activity and promotion by Co, Carbon, 39, 2023-2034.

Kaluža L., Vít Z., Zdražil M., 2005, Preparation and properties of filled monolayer of MoO_3 deposited on Al_2O_3 supports by solvent-assisted spreading, Appl. Catal. A: General, 282, 247-253.

Kaluža L., Zdražil M., 2009, Slurry impregnation of ZrO_2 extrudates: Controlled eggshell distribution of MoO3, hydrodesulfurization activity, promotion by Co, Catal. Lett., 127, 368-376.

Kaluža L., Zdražil M., Gulková D., Vít Z., 2013, The influence of the chelating agent nitrilotriacetic acid on promotion of hydrodesulfurization activity by Co in CoMo catalysts prepared on Al_2O_3, C, and ZrO_2 supports, Chemical Engineering Transactions, 32, 841-846.

Kolaczkowski S.T., 2003, Measurement of effective diffusivity in catalyst-coated monoliths, Catal. Today, 83, 85-95.

Kučera E., 1965, Contribution to the theory of chromatography: linear non-equilibrium elution chromatography, J. Chromatogr., 19, 237-248.

Leliveld R.G., Eijsbouts S.E., 2008, How a 70-year-old catalytic refinery process is still ever dependent on innovation, Catal. Today, 130, 183-189.

Schneider P., Multicomponent isothermal diffusion and forced flow of gases in capillaries, 1978, Chem. Eng. Sci., 33, 1311-1319.

Schneider P., 1984, Time-domain expression for impulse response (chromatographic) curve for the Kubín-Kučera model of adsorption column, Chem. Eng. Sci., 39, 927-929.

Schneider P., 1995, Adsorption isotherm of microporous-mesoporous solids revisited, Appl. Catal. A: General, 129, 157–165.

Schneider P., Hudec P., Šolcová O., 2008, Pore-volume and surface area in microporous-mesoporous solids, Micro. Meso. Matter., 115, 491–496.

Šolcová O., Soukup K., Schneider P., 2006, Diffusion coefficients and other transport characteristics of peculiarly shaped porous materials in the single pellet-string column, Micro. Meso. Mat., 91 100-1006.

Toulhoat H., Raybaud. P., 2013, Catalysis by Transition Metal Sulphides, Editions Technip, Paris, France.